Ionic photofragmentation and photoionization of dimethyl ether in the VUV and soft X-ray regions (8.5–80 eV) – Absolute oscillator strengths for molecular and dissociative photoion…

ARTICLE *in* CHEMICAL PHYSICS · AUGUST 2001

Impact Factor: 1.65 · DOI: 10.1016/S0301-0104(01)00402-5

3 AUTHORS, INCLUDING:

C.E. Brion
University of British Columbia - Vanco…

209 PUBLICATIONS **6,652** CITATIONS

SEE PROFILE

ELSEVIER

Chemical Physics 270 (2001) 319–332

Chemical Physics

www.elsevier.com/locate/chemphys

Ionic photofragmentation and photoionization of dimethyl ether in the VUV and soft X-ray regions (8.5–80 eV) – absolute oscillator strengths for molecular and dissociative photoionization

Renfei Feng, Glyn Cooper, C.E. Brion *

Department of Chemistry, University of British Columbia, 2036 Main Mall, Vancouver, BC, Canada V6T 1Z1

Received 5 March 2001

Abstract

The branching ratios for molecular and dissociative photoionization of dimethyl ether (CH_3OCH_3, DME) have been measured in the VUV and soft X-ray regions using dipole (e,e+ion) coincidence spectroscopy (~1 eV FWHM) at equivalent photon energies from the first ionization threshold up to 80 eV. The absolute partial oscillator strengths (cross-sections) for molecular and dissociative photoionization have been determined from recently published absolute photoabsorption oscillator strength data [R. Feng, G. Cooper, C.E. Brion, Chem. Phys. 260 (2000) 391] together with the photoionization branching ratios and the (multi-dissociative-corrected) photoionization efficiency obtained from time-of-flight mass spectra reported in the present work. No stable multiply charged molecular ion(s) from DME have been found in the present work. However, the fact that the photoionization efficiency has been measured as greater than unity above ~30 eV indicates the existence of multi-dissociative products from Coulomb explosion of multiply charged ions. Appearance potentials of all ion products from DME are also reported. The presently reported results are compared with the previously published data where possible.

1. Introduction

Molecular photoionization and ionic photofragmentation processes are of fundamental importance in understanding the interaction between photons and molecules and also the action of ionizing radiation on matter. Such information finds application in a large number of scientific contexts, including studies in aeronomy, astrophysics, planetary science, fusion, and radiation chemistry, physics, and biology [1]. Accurate absolute oscillator strengths (cross-sections) for total photoabsorption, total photoionization, partial photoionization, and ionic photofragmentation processes are required over wide spectral regions for use in modeling studies. Similarly, experimental total and partial oscillator strength data can be used to evaluate theoretical concepts and computational approximations used in modeling molecular photoabsorption, photoionization and ionic photofragmentation processes [1].

Dimethyl ether (CH_3OCH_3, DME) is a simple but chemically important organic molecule. It has

* Corresponding author. Tel.: +1-604-822-3266; fax: +1-604-822-2847.

E-mail address: brion@chem.ubc.ca (C.E. Brion).

0301-0104/01/$ - see front matter
PII: S0301-0104(01)00402-5

found many uses in chemistry and industry [2]. As described earlier [2], photoabsorption studies of DME have been previously reported in limited energy ranges [3–9] using Beer–Lambert law based optical methods. Recently, new very accurate and much wider (energy) range absolute photoabsorption oscillator strength measurements [2] have been reported at both high and low energy resolution in the UV, VUV and soft X-ray regions (5–32 eV and 5–200 eV, respectively) using fast electron impact based dipole (e,e) methods. This work [2] has made the present quantitative experimental study of the ionic photofragmentation and photoionization of DME possible.

Photoionization processes of DME have been previously studied by photoionization [10,11], photoelectron (HeI and HeII) [12–26] and Penning ionization [27] spectroscopies. These studies were in general concerned with the measurement of ionization potentials (IPs) and their assignments to the associated outer valence orbitals. Similar information, such as the binding energy spectra [28, 29] and orbital assignments for the valence shell ionization spectrum of DME, have also been measured using electron momentum spectroscopy (EMS). Quantitative studies of photoionization quantum yields [30,31] and total photoionization cross-sections [31] have only been reported in the limited energy ranges ~9.84–11.8 eV [30] and ~13.5–23.8 eV [31] using synchrotron radiation. Some photodissociation processes and dynamics of DME have been previously studied using electron impact (EI) [32–38] and threshold photoelectron–photoion coincidence (PEPICO) [39] spectroscopies. These studies were concerned with the determination of the appearance potentials (APs) and the heats of formation for a number of ions produced from DME. Relative photoionization yield curves for a few ions from DME in the limited energy range (9.4–18 eV) and some APs have also been reported earlier using photoionization mass spectrometry (PIMS) [11]. No quantitative studies of ionic photofragmentation and photoionization cross-sections (oscillator strengths) have previously been reported for DME, to the best of our knowledge.

In the present work, dipole (e,e+ion) spectroscopy, which is now well known as a reliabl alternative to PIMS [1], has been used to determined the photoion branching ratios of DME in the equivalent photon energy range 8.5–80 eV using time-of-flight mass spectrometry (TOFMS). The ion APs for the molecular and fragment ions as obtained from time-of-flight (TOF) mass spectra are also reported. Since a very accurate wide range absolute photoabsorption oscillator strength spectrum has recently been reported from this laboratory for DME [2], the absolute partial oscillator strengths for molecular and dissociative photoionization can now be determined from these data together with the photoionization branching ratios and the (multi-dissociative-corrected) photoionization efficiency obtained from the TOF mass spectra reported in the present work. The present work which provides absolute intensity measurements also considerably extends the scope and energy range of the previous (relative) measurements [11,39]. The presently reported results are compared with previously published data where possible.

2. Experimental

The instrumentation and experimental procedures employed to obtain absolute photoabsorption oscillator strengths and partial photoionization oscillator strengths for molecular and dissociative photoionization, using a combination of TOFMS and electron energy loss spectroscopy (EELS) in the dipole (e,e+ion) coincidence spectrometer, are similar to those used in our recent studies of H_2S [40,41] and OCS [42,43]. Therefore only a brief description will be given here.

The absolute photoabsorption oscillator strengths for DME (5–200 eV) were obtained as described earlier [2] by Bethe–Born conversion and valence-shell TRK sum-rule normalization of background subtracted dipole (e,e) electron energy loss measurements, collected at a mean scattering angle of zero degree and high electron impact energy (8 keV) in the non-coincident forward (e,e) channel of the dipole (e,e+ion) spectrometer [40, 41], i.e., the low resolution (~1 eV FWHM) dipole (e,e) mode [1]. These absolute photoabsorption results have been reported and discussed in our

recently published work [2]. TOF mass spectra at selected equivalent photon energies were obtained by detection of the forward scattered electrons at a particular energy loss (photon energy) in coincidence with positive ions extracted at 90° to the incident electron beam using both channels of the spectrometer, i.e., the dipole (e,e+ion) mode [1,40,41]. An improved ion detector using a double Chevron microchannel plate (MCP) [44] assembly together with a single stop time-to-amplitude converter (TAC) was used for the TOFMS measurements. The ion extraction voltages and TOF analyzer lens system ensure uniform collection of ions with excess kinetic energies of fragmentation up to 20 eV [41]. This uniform collection is essential if accurate branching ratios and partial oscillator strengths are to be obtained for molecular and dissociative photoionization processes, especially when energetic fragment ions are formed. The ion yields were corrected for multiplier sensitivity as a function of mass to charge ratio [44]. The present TOFMS measurements were obtained at an energy resolution of ~1 eV FWHM over the equivalent photon energy regions 8.5–30, 30–50, and 55–80 eV at intervals of 0.5, 2 and 5 eV, respectively. The branching ratios for the individual ions were obtained by integrating the peaks of the background subtracted TOF mass spectra and normalizing to a total of 100%. The photoabsorption oscillator strengths used in the present work for calculating the partial photoionization oscillator strengths have been reported in our recently published work [2] using the same instrumentation used in the dipole (e,e) mode. Multi-dissociative photoionization processes occurring at higher energies are considered in determining the photoionization efficiencies [43].

The sample of DME, obtained commercially from Matheson Gas Products Ltd., was thoroughly degassed by freeze–pump–thaw cycles. No impurity peaks were observed in the TOF mass spectra after this purification. The present energy scale (low resolution) was calibrated by comparing the low resolution photoabsorption oscillator strength spectrum with the high resolution photoabsorption oscillator strength spectrum (convoluted with 1 eV FWHM Gaussian) and therefore the accuracy is expected to be better than ±0.1 eV [2]. The reproducibilities of the branching ratios and the uncertainties of the absolute partial oscillator strength scale in the present work are estimated to approximately ±5% for the intense $m/z = 46,45,31,29,15,1$ ions, ±15% for $m/z = 44$, 43,32,20,18,17,16 ions and ±20% for $m/z = 42$, 41,28,27,14,13,12,2 ions. The maximum uncertainties of the APs for these groups of ions determined in the present work are estimated to be ±1, ±2 and ±3 eV, respectively.

3. Results and discussion

3.1. Electronic structure of dimethyl ether

DME is a simple organic molecule belonging to the C_{2v} molecular point group. The ground state independent particle electron configuration can be written as:

core: $(1a_1)^2(1b_2)^2(2a_1)^2$,
valence shell: $(3a_1)^2(2b_2)^2(4a_1)^2(1b_1)^2(5a_1)^2(3b_2)^2$ $(1a_2)^2(4b_2)^2(6a_1)^2(2b_1)^2$.

The photoion branching ratio curves and the photoionization oscillator strength spectrum of DME are conveniently discussed with reference to this electron configuration.

The ionization energies for the valence orbitals of DME have been determined by PES [12–26] and EMS [28,29] measurements to be: 10.1 eV ($2b_1$), 11.9 eV ($6a_1$), 13.4 eV ($4b_2$), 14.2 eV ($1a_2$), 16.2 eV ($3b_2$), 16.2 eV ($5a_1$), 16.2 eV ($1b_1$), 21.2 eV ($4a_1$), 23.4 eV ($2b_2$) and 32.3 eV ($3a_1$). The ionization spectrum of the inner valence orbitals $2b_2$ and $3a_1$ is split into several peaks, in addition to the main peaks at 23.4 and 32.3 eV, by extensive many-body (electron correlation) effects over the energy range ~30–50 eV [28,29].

3.2. Time-of-flight mass spectra and photoion branching ratios

TOF mass spectra of DME were obtained in the equivalent photon energy (energy loss) range 8.5–80 eV. Analysis of these data provides information concerning the molecular and dissociative

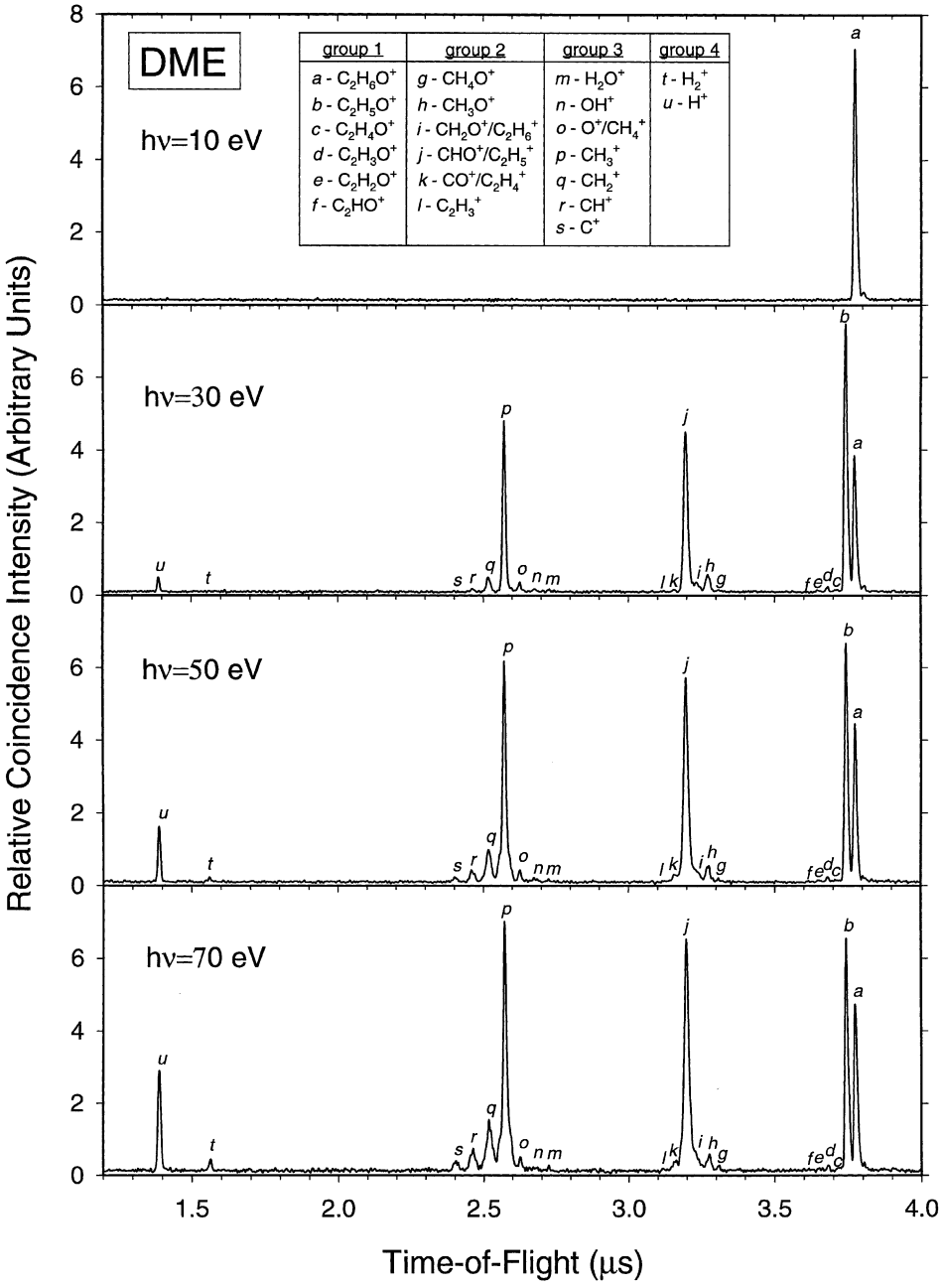

Fig. 1. TOF mass spectra of DME obtained at equivalent photon energies of 10, 30, 50 and 70 eV.

photoionization channels resulting from valence shell photoabsorption by DME. Fig. 1 shows the TOF mass spectra measured at equivalent photon energies of 10, 30, 50 and 70 eV. Four groups of photoion peaks were detected in the TOF mass spectra. They correspond to: (1) $C_2H_6O^+$, $C_2H_5O^+$, $C_2H_4O^+$, $C_2H_3O^+$, $C_2H_2O^+$ and C_2HO^+ (group 1, $m/z = 46,45,44,43,42,41$); (2) CH_4O^+,

CH_3O^+, $CH_2O^+/C_2H_6^+$, $CHO^+/C_2H_5^+$, $CO^+/C_2H_4^+$, $C_2H_3^+$ (group 2, $m/z = 32,31,30,29,28,27$); (3) H_2O^+, OH^+, CH_4^+/O^+, CH_3^+, CH_2^+, CH^+, C^+ (group 3, $m/z = 18,17,16,15,14,13,12$); and (4) H_2^+, H^+ (group 4, $m/z = 2,1$). It can be seen (Fig. 1) that the molecular ion $C_2H_6O^+$ and the fragments ions $C_2H_5O^+$, $CHO^+/C_2H_5^+$, CH_3^+ and H^+ are the dominant ionic products for valence shell photoionization/photofragmentation of DME. No stable multiply charged molecular or fragment ions from DME were observed in the present work. Contributions from the products of dissociative double/triple photoionization or Coulomb explosion, which can be investigated by photoion–photoion coincidence (PIPICO) or photoelectron–photoion–photoion (PEPIPICO) techniques, cannot be unambiguously identified in the singly charged ion yields measured in the present work. However, the changes in the shapes of the CH_3^+ TOF peaks with photon energy clearly indicates that some of these ions originate from those (dissociative multi-photoionization or Coulomb explosion) processes at higher photon energies. These types of ion products usually carry much more kinetic energy than direct photoionization/photodissociation prod-ucts, and therefore result in broader TOF distributions. These broader components ("wings") clearly appear in the CH_3^+ peak (p peak) of the TOF spectra above ~50 eV photon energy (see Fig. 1). The very small peaks at $m/z = 47$ (i.e., just above the main $C_2H_6O^+$ peak (a)) is due to the ^{13}C carbon isotope (natural abundance ~1%).

Photoion branching ratios (% of total ionization) for the molecular and dissociative ions (four groups) from DME have been determined as percentages of the total photoionization from integration of the peaks in the background subtracted TOF mass spectra at each energy. They are shown diagrammatically in Figs. 2–5 for ion groups 1–4 respectively. The numerical values for the branching ratio for DME can be calculated from the oscillator strength data given in Table 2 by dividing the partial photoionization oscillator strength for the ion of interest by the total photoionization oscillator strength (sum of all the ions) at each energy. The dominant ion products, i.e. those have branching ratios higher than 10%, are $C_2H_6O^+$, $C_2H_5O^+$, $CHO^+/C_2H_5^+$ and CH_3^+.

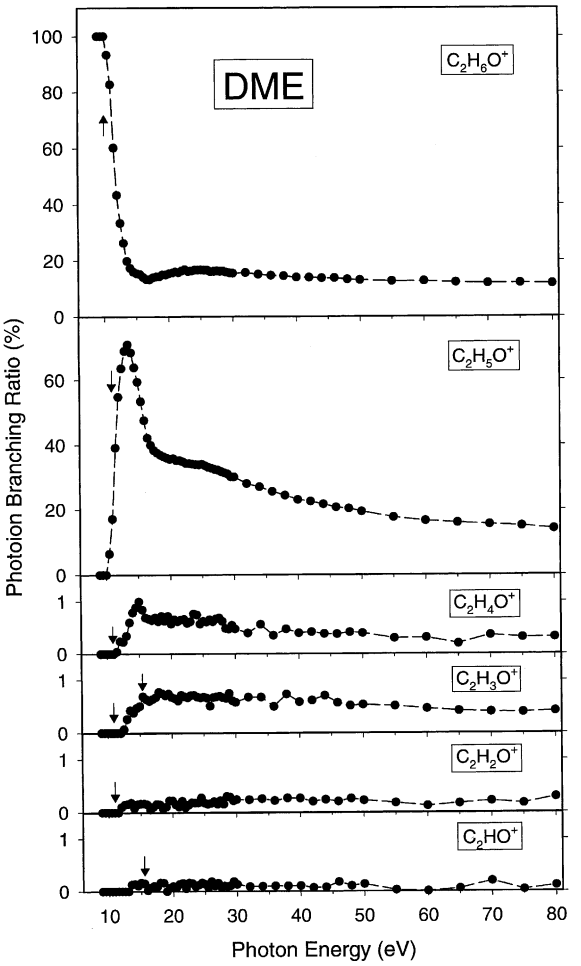

Fig. 2. Branching ratios for molecular and dissociative photoionization (solid circles with dashed lines) for group 1 ions ($m/z = 46,45,43,42,41$) of DME in the equivalent photon energy region 10–80 eV. The vertical arrows indicate expected APs estimated using thermodynamic data for enthalpies of formation of ions and neutrals [45] (see text for details).

The ion products CH_3O^+, CH_2^+, CH^+ and H^+ have branching ratios in the ~1–10% range. Other ion products ($C_2H_4O^+$, $C_2H_3O^+$, $C_2H_2O^+$, C_2HO^+, CH_4O^+, $CH_2O^+/C_2H_6^+$, $CO^+/C_2H_4^+$, $C_2H_3^+$, H_2O^+, OH^+, O^+, C^+ and H_2^+) have branching ratios that are only ~1% or lower. It can be noted that the branching ratios of $CHO^+/C_2H_5^+$, CH_3^+, CH_2^+, CH^+, C^+, H_2^+ and H^+ increase significantly with increase in photon energy. These changes may be due to the onset of multi-dissociative processes caused by Coulomb explosion of unstable multiply

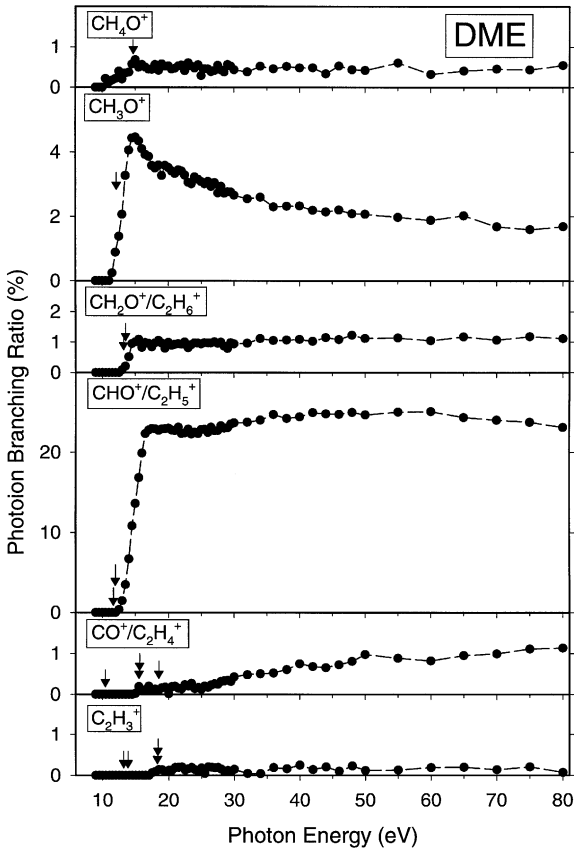

Fig. 3. Branching ratios for molecular and dissociative photoionization (solid circles with dashed lines) for group 2 ions ($m/z = 32,31,30,29,28,27$) of DME in the equivalent photon energy region 10–80 eV. The vertical arrows indicate expected APs estimated using thermodynamic data for enthalpies of formation of ions and neutrals [45] (see text for details).

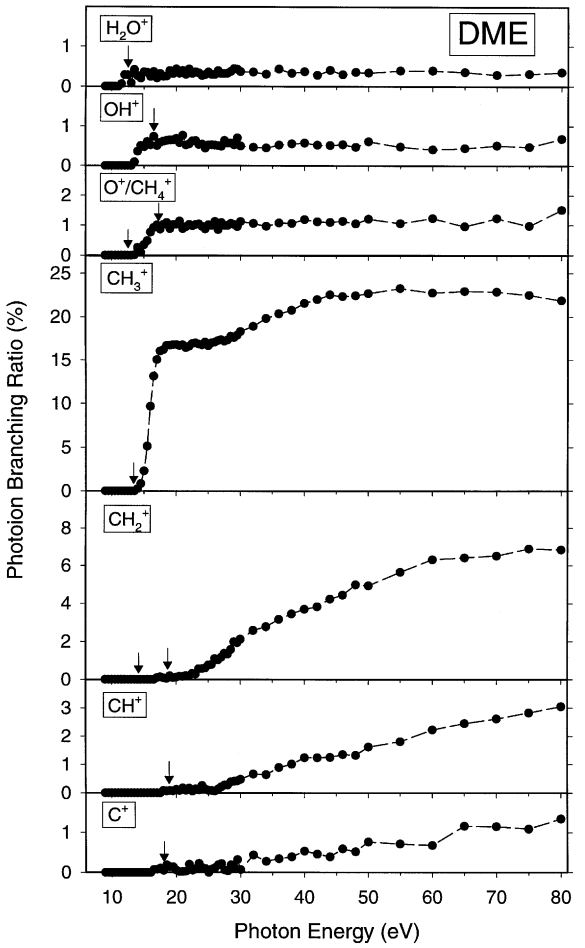

Fig. 4. Branching ratios for molecular and dissociative photoionization (solid circles with dashed lines) for group 3 ions ($m/z = 18,17,16,15,14,13,12$) of DME in the equivalent photon energy region 10–80 eV. The vertical arrows indicate expected APs estimated using thermodynamic data for enthalpies of formation of ions and neutrals [45] (see text for details).

charged ions, evidence for which has already been mentioned in regard to the peak broadening in TOF spectra at higher energies (see Fig. 1). Further evidence for such processes comes from the photoionization efficiency data (see next section and also Fig. 6 and Table 2).

3.3. Appearance potentials and possible dissociative processes

The first IP and the APs of fragment ions from DME were determined in the present work by extrapolating the related branching ratios to zero and also taking into account the experimental energy resolution (~1 eV FWHM) of the instrumentation. The ionization and AP data are shown in Table 1 together with the previously published values for comparison [11,32–39], which are only available for the dominant ion products $C_2H_6O^+$, $C_2H_5O^+$, CH_3O^+, $CHO^+/C_2H_5^+$ and CH_3^+. It is found that the presently determined APs for the dominant ion products $C_2H_6O^+$, $C_2H_5O^+$, CH_3O^+, $CHO^+/C_2H_5^+$ and CH_3^+ are generally in reasonable agreement with other previously published data from PEPICO [39], electron-impact [32–38] and

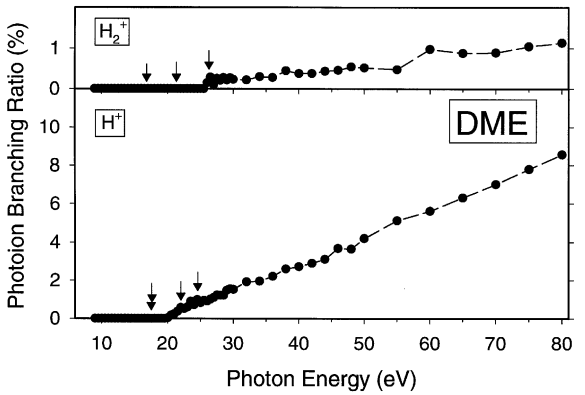

Fig. 5. Branching ratios for molecular and dissociative photoionization (solid circles with dashed lines) for group 4 ions ($m/z = 2,1$) of DME in the equivalent photon energy region 10–80 eV. The vertical arrows indicate expected APs estimated using thermodynamic data for enthalpies of formation of ions and neutrals [45] (see text for details).

PIMS [11] experiments, within the estimated experimental errors.

The possible dissociative channels and their APs estimated from thermodynamic data [45] are also given in Table 1. It should be noted that these calculated values assume zero kinetic energy of fragmentation and as a result the actual thresholds may be higher than the estimated values. The estimated values of the APs are shown by the vertical arrows in Figs. 2–5 (also in Figs. 7–10) to indicate the possible dissociative channels. From Table 1, it is found that, for the dominant ion products, the estimated APs show reasonable agreement with the presently reported data and the other experimental values [11,32–39] for $C_2H_6O^+$, $C_2H_5O^+$ and CH_3O^+, but are somewhat lower than experiment for $CHO^+/C_2H_5^+$ and CH_3^+ (see Table 1), which are more likely to have appreciable kinetic energies of fragmentation. For the other ion products, there are no previously published experimental data, and therefore only the calculated APs are listed in Table 1 for comparison with the presently reported data.

3.4. Photoionization efficiencies and total photoionization oscillator strengths

In the dipole (e,e+ion) experiment, the ratio of the total coincident ion counts to the forward scattered energy loss counts at each energy gives the relative photoionization efficiency [1]. In the present work for DME, the relative photoionization efficiency reaches a plateau from ~18 to ~30 eV. Making the reasonable assumption that the photoionization efficiency is unity in this energy region [1], we obtain the measured photoionization efficiency η_i (also known as ionization quantum yield) from the first IP up to 80 eV, which is shown as the solid circles in the upper panel of Fig. 6. The previously published photoionization efficiency data from photoionization measurements [30,31] are compared with the present data in those limited energy ranges where previous data are available (~9.84–11.8 eV [30] and ~13.5–18 eV [31], respectively) in the insert on the upper panel in

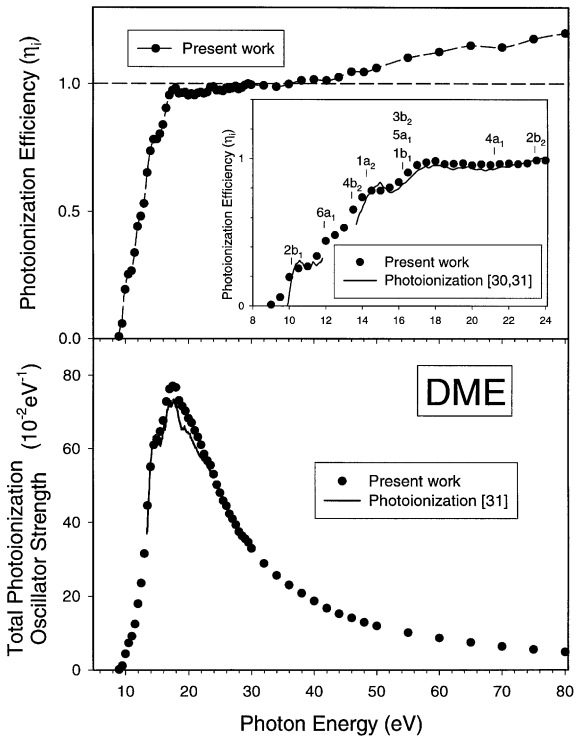

Fig. 6. Presently determined photoionization efficiencies (upper) and absolute total photoionization oscillator strengths (lower) for DME in the equivalent photon energy region 10–80 eV. The solid lines show previously reported data from photoionization measurements [30,31]. The vertical lines indicate the IPs for the valence shell orbitals [12–26,28,29] (see text for details).

Table 1
Experimental and calculated APs for the positively charged ions produced from DME with possible processes

Product	Possible process	Ion appearance potential (eV)									
		Calculated[a]	Dipole (e,e+ion) (this work)	PEPICO [39]	Electron impact						PIMS
					[36]	[32]	[33]	[34]	[35]	[37]	[38]	[11]
$C_2H_6O^+$	Ionization	10.03	9.5[b]	10.025	10.12	9.95						10.01
$C_2H_5O^+$	$C_2H_5O^+ + H$	10.98	11.0[b]	11.115	11.55	10.99	10.99	11.23	10.7	11.42		11.04
$C_2H_4O^+$	$C_2H_4O^+ + H_2$	10.88	12.0[c]									
	$C_2H_4O^+ + 2H$	15.40										
$C_2H_3O^+$	$C_2H_3O^+ + H + H_2$	10.93	13.0[c]									
	$C_2H_3O^+ + 3H$	15.45										
$C_2H_2O^+$	$C_2H_2O^+ + 2H_2$	11.02	12.5[d]									
C_2HO^+	$C_2HO^+ + 2H_2 + H$	15.53	14.0[d]									
CH_4O^+	$CH_4O^+ + CH_2$	14.70	13.5[c]									
CH_3O^+	$CH_3O^+ + CH_3$	12.13	12.0[b]	$\leqslant 11.85$	12.42		$\leqslant 11.8$				11.95	13.35
CH_2O^+/	$CH_2O^+ + CH_3 + H$	13.52										
$C_2H_6^+$	$C_2H_6^+ + O$	13.23	13.5[c]									
CHO^+/	$CHO^+ + CH_3 + H_2$	11.97										
$C_2H_5^+$	$C_2H_5^+ + OH$	11.66	13.0[b]	$\leqslant 12.85$	13.96							
CO^+/	$CO^+ + CH_3 + H_2 + H$	18.54										
$C_2H_4^+$	$C_2H_4^+ + H_2O$	10.45	15.5[d]									
	$C_2H_4^+ + O + H_2$	15.54										
	$C_2H_4^+ + H + OH$	15.62										
$C_2H_3^+$	$C_2H_3^+ + H_2O + H$	13.19	18.0[d]									
	$C_2H_3^+ + OH + H_2$	13.84										
	$C_2H_3^+ + O + H + H_2$	18.28										
	$C_2H_3^+ + OH + 2H$	18.36										
H_2O^+	$H_2O^+ + C_2H_4$	12.55	12.0[c]									
OH^+	$OH^+ + C_2H_5$	16.53	14.0[c]									
O^+/CH_4^+	$O^+ + C_2H_6$	17.24										
	$CH_4^+ + CH_2O$	12.53	14.0[c]									
CH_3^+	$CH_3^+ + CH_3O$	13.40	14.5[b]	$\leqslant 14.4$							14.93	14.4
	$CH_3^+ + CH_2O + H$	14.37										
CH_2^+	$CH_2^+ + CH_4O$	14.17	17.5[d]									
	$CH_2^+ + CH_3O + H$	18.68										
CH^+	$CH^+ + CH_3O + H_2$	18.89	18.5[d]									
	$CH^+ + CH_4O + H$	18.89										
C^+	$C^+ + CH_4O + H_2$	18.08	17.0[d]									
H_2^+	$H_2^+ + C_2H_2O + H_2$	16.84	26.5[d]									
	$H_2^+ + C_2H_4O$	–										
	$H_2^+ + C_2H_2O + 2H$	21.36										
	$H_2^+ + C_2H_4O^+$	26.31										
H^+	$H^+ + C_2H_5O$	17.64	20.5[b]									
	$H^+ + C_2H_5O^+$	24.57										
	$H^+ + C_2H_4O + H/H^+$	–										
	$H^+ + C_2H_3O + H_2$	17.51										
	$H^+ + C_2H_3O + 2H$	22.02										

[a] Values calculated using thermodynamic data for the enthalpies of formation of ions and neutrals (taken from Ref. [45]) assuming zero kinetic energy of fragmentation.
[b] ±1 eV.
[c] ±2 eV.
[d] ±3 eV.

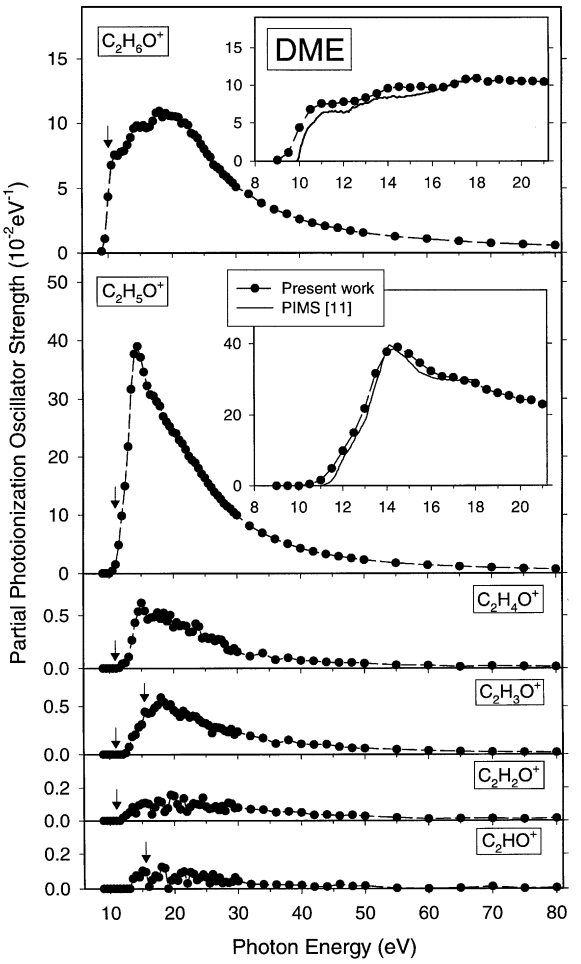

Fig. 7. Absolute partial oscillator strengths for the molecular and dissociative photoionization of group 1 ($m/z = 46,45,44, 43,42,41$) ions from DME in the equivalent photon energy region 10–80 eV. Previously reported relative ion yield data [11] have been normalized to the present work and are shown as solid lines for comparison. The vertical arrows indicate expected APs estimated using thermodynamic data for enthalpies of formation of ions and neutrals [45]. See text for details.

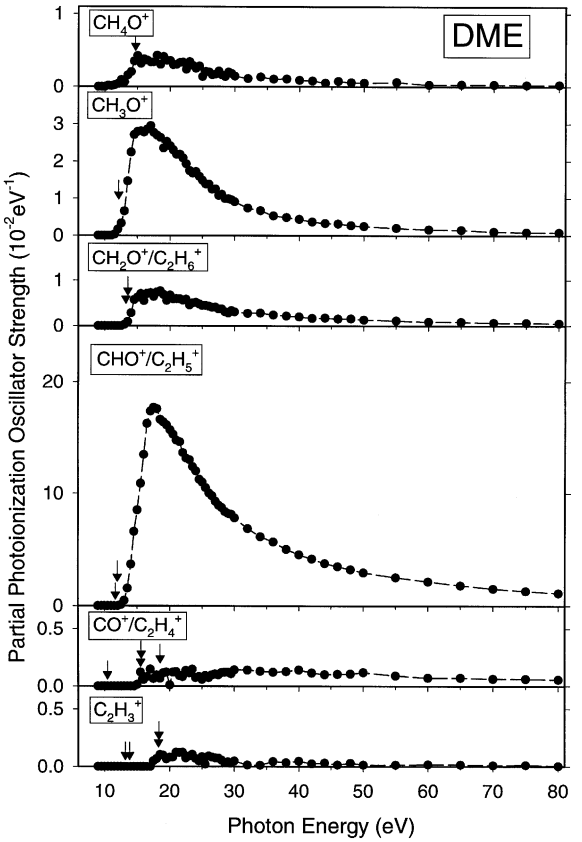

Fig. 8. Absolute partial oscillator strengths for the molecular and dissociative photoionization of group 2 ($m/z = 32,31,30, 29,28,27$) ions from DME in the equivalent photon energy region 10–80 eV. The vertical arrows indicate expected APs estimated using thermodynamic data for enthalpies of formation of ions and neutrals [45] (see text for details).

Fig. 6. Despite the differences in energy resolution, excellent agreement is found between these data sets. The IPs of DME from PES [12–26] and EMS [28,29] are shown on the insert to Fig. 6. It can be seen that the photoionization efficiency curve shows features which correspond to many of IPs. The presently measured η_i data is also presented numerically in Table 2. It can be seen that the photoionization efficiency η_i exceeds unity above ~30 eV. In this higher energy region, dissociation of multiply charged ions may be expected to occur by instantaneous Coulomb explosion [43]. In principle, when dissociation of multiply charged ions occurs, the heavier ion(s) is(are) not counted by the experiment, because the lighter (faster) ion is the one that stops the (single-stop) TAC. However, in practice, since typical ion detection efficiencies are very much less than 100% [44], significant probability for detecting the heavier ions remains. In these circumstances, the measured photoionization efficiency is therefore expected to

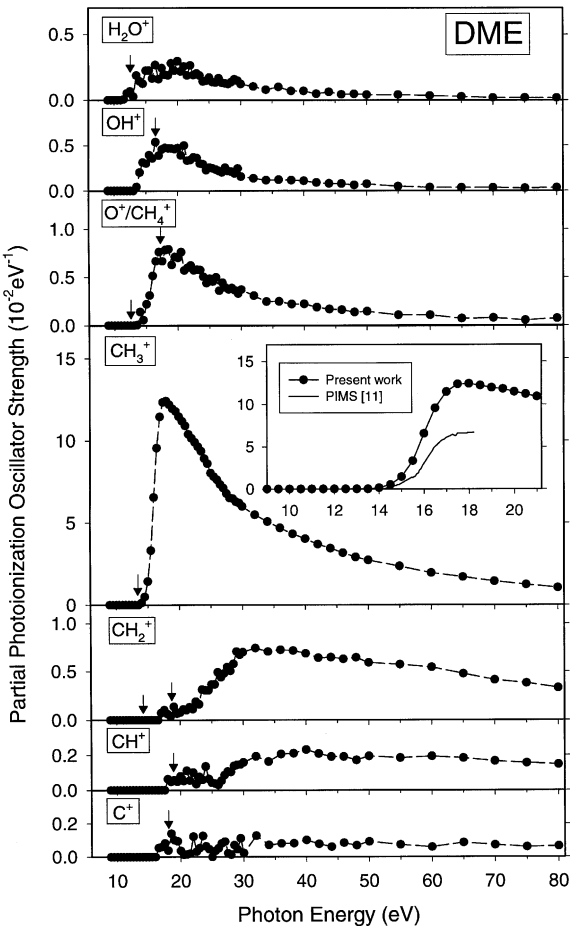

Fig. 9. Absolute partial oscillator strengths for the molecular and dissociative photoionization of group 3 ($m/z = 18,17,16,15,14,13,12$) ions from DME in the equivalent photon energy region 10–80 eV. Previously reported relative ion yield data [11] have been normalized to the present work and are shown as solid line for comparison. The vertical arrows indicate expected APs estimated using thermodynamic data for enthalpies of formation of ions and neutrals [45]. See text for details.

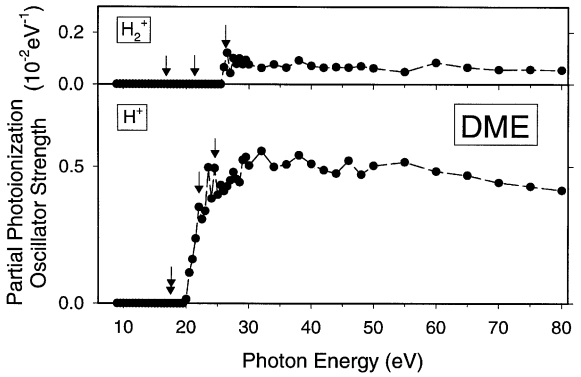

Fig. 10. Absolute partial oscillator strengths for the molecular and dissociative photoionization of group 4 ($m/z = 2,1$) ions from DME in the equivalent photon energy region 10–80 eV. The vertical arrows indicate expected APs calculated using thermodynamic data for enthalpies of formation of ions and neutrals [45] (see text for details).

be greater than unity when dissociation of multiply charged ions occurs. Since the overall ion detection efficiency in the present dipole (e,e+ion) spectrometer is in fact only ~10% [44], the probabilities for detection of the lighter and heavier ions from multiply dissociative processes are almost the same (i.e., for the lightest ion it is ~10%; then for the next heavier ion it is $\sim(100\% - 10\%) \times 10\% = 9\%$, then $\sim(100\% - 10\%)^2 \times 10\% = 8.1\%$, etc.). As such, the dipole (e,e+ion) spectrometer employed in the present work can essentially give the correct photoionization efficiency η_i, even in the higher energy (inner valence) regions where Coulomb explosion of multiply charged ions is expected to occur (i.e. above ~30 eV).

Absolute total photoionization oscillator strengths have been obtained from the product of the recently reported, very accurate absolute photoabsorption oscillator strengths [2] and the presently measured photoionization efficiencies (Section 3.4 above) in the equivalent photon energy range 8.5–80 eV. These results are shown diagrammatically in the lower panel of Fig. 6 (as solid circles) and are given numerically in Table 2. The previously published photoionization data from ~13.5–23.8 eV [31] are also shown for comparison as solid lines in the figure. These two data sets are in very good agreement, although the previously published photoionization data [31] are very slightly lower than the present data near the maxima. The small differences in shape are probably exist due to differences in energy resolutions between the two experiments. Above ~30 eV, the presently determined absolute total photoionization oscillator strengths essentially decrease monotonically.

Table 2
Absolute differential oscillator strengths for the molecular and dissociative photoionization of dimethyl ether

Energy (eV)	Oscillator strength (10^{-2} eV^{-1})																					η_i
	Total	Partial photoionization																				
		$C_2H_6O^+$	$C_2H_5O^+$	$C_2H_4O^+$	$C_2H_3O^+$	$C_2H_2O^+$	C_2HO^+	CH_4O^+	CH_3O^+	$C_2H_6^+$ CH_2O^+	$C_2H_5^+$ CHO^+	$C_2H_4^+$ CO^+	$C_2H_3^+$	H_2O^+	OH^+	CH_4^+ O^+	CH_3^+	CH_2^+	CH^+	C^+	H_2^+	H^+	
8.5	0.000																					0.00
9.0	0.128	0.128																				0.01
9.5	1.115	1.115																				0.06
10.0	4.364	4.364																				0.19
10.5	7.286	6.801	0.470					0.015														0.25
11.0	9.156	7.580	1.564					0.011														0.27
11.5	12.47	7.517	4.891	0.005				0.021	0.031					0.008								0.34
12.0	17.96	7.800	9.844	0.042		0.018		0.038	0.160					0.052								0.44
12.5	23.53	7.886	14.96	0.053	0.017	0.035		0.092	0.326		0.088			0.067								0.48
13.0	31.60	8.344	21.78	0.107	0.082	0.051		0.063	0.653	0.028	0.468			0.027								0.53
13.5	44.62	8.885	31.62	0.266	0.188	0.083	0.058	0.156	1.466	0.094	1.571			0.188	0.043	0.006						0.65
14.0	55.12	9.590	37.71	0.433	0.209	0.046	0.077	0.204	2.238	0.287	3.705			0.145	0.202	0.140	0.134					0.74
14.5	61.06	9.807	39.01	0.539	0.285	0.095	0.066	0.348	2.709	0.578	6.619			0.126	0.313	0.058	0.510					0.78
15.0	62.53	9.659	37.15	0.622	0.313	0.105	0.104	0.425	2.792	0.626	8.529	0.014		0.225	0.300	0.221	1.447					0.78
15.5	64.71	9.834	34.60	0.544	0.443	0.109	0.096	0.317	2.811	0.705	10.88	0.120		0.226	0.394	0.311	3.320					0.80
16.0	67.68	9.609	32.25	0.464	0.428	0.102	0.012	0.377	2.776	0.557	13.46	0.056		0.166	0.357	0.515	6.547					0.84
16.5	72.82	9.725	30.73	0.482	0.435	0.039	0.051	0.361	2.860	0.713	16.26	0.080		0.267	0.538	0.669	9.558			0.054		0.91
17.0	76.24	10.16	30.50	0.487	0.482	0.083	0.076	0.337	2.948	0.726	17.37	0.145		0.161	0.389	0.764	11.47	0.072		0.061		0.96
17.5	77.05	10.81	29.54	0.528	0.514	0.123	0.066	0.338	2.765	0.649	17.70	0.064	0.048	0.244	0.457	0.669	12.35	0.102		0.083		0.97
18.0	76.66	10.93	28.78	0.470	0.591	0.115	0.126	0.429	2.692	0.741	17.58	0.096	0.069	0.192	0.475	0.786	12.43	0.063	0.064	0.038		0.98
18.5	73.11	10.47	27.00	0.524	0.543	0.054	0.119	0.303	2.631	0.768	16.63	0.067	0.104	0.189	0.468	0.791	12.21	0.038	0.049	0.141		0.96
19.0	71.57	10.76	26.08	0.445	0.504	0.076	0.000	0.413	2.350	0.689	16.40	0.112	0.098	0.281	0.467	0.630	11.96	0.136	0.058	0.101		0.96
19.5	70.30	10.58	25.31	0.504	0.519	0.157	0.048	0.360	2.524	0.563	16.14	0.119	0.066	0.225	0.460	0.713	11.80	0.066	0.049	0.095		0.97
20.0	68.29	10.54	24.29	0.389	0.459	0.150	0.066	0.357	2.406	0.674	15.71	0.010	0.081	0.296	0.471	0.703	11.47	0.079	0.081	0.037		0.015	0.95
20.5	67.12	10.52	24.04	0.436	0.433	0.101	0.047	0.299	2.295	0.596	15.30	0.119	0.084	0.219	0.391	0.762	11.20	0.109	0.053	0.012		0.111	0.96
21.0	65.02	10.44	22.91	0.400	0.393	0.070	0.090	0.302	2.177	0.600	14.77	0.124	0.123	0.257	0.500	0.573	10.91	0.103	0.112	0.015		0.160	0.96
21.5	63.23	9.978	22.26	0.407	0.450	0.136	0.099	0.330	2.182	0.595	14.62	0.090	0.121	0.188	0.332	0.599	10.40	0.131	0.056	0.020		0.236	0.96
22.0	61.08	10.03	21.26	0.401	0.416	0.056	0.030	0.334	2.085	0.564	13.64	0.081	0.123	0.264	0.340	0.624	10.14	0.114	0.103	0.123		0.350	0.97
22.5	58.54	9.851	20.11	0.340	0.386	0.083	0.095	0.237	1.927	0.583	13.13	0.133	0.075	0.190	0.369	0.572	9.902	0.187	0.035	0.032		0.306	0.96
23.0	56.74	9.217	19.44	0.346	0.399	0.106	0.085	0.341	1.741	0.462	12.99	0.113	0.091	0.204	0.361	0.580	9.639	0.162	0.077	0.053		0.336	0.97
23.5	55.54	9.093	18.97	0.421	0.392	0.101	0.050	0.290	1.679	0.504	12.37	0.144	0.105	0.187	0.299	0.576	9.358	0.313	0.060	0.126		0.497	0.99
24.0	53.14	8.858	18.04	0.394	0.358	0.097	0.064	0.250	1.718	0.516	11.97	0.072	0.071	0.143	0.291	0.506	8.904	0.305	0.136	0.064		0.381	0.99
24.5	50.33	8.388	17.06	0.284	0.331	0.139	0.081	0.280	1.593	0.484	11.24	0.082	0.047	0.147	0.226	0.438	8.593	0.306	0.065	0.046		0.495	0.97
25.0	48.11	8.036	16.37	0.297	0.323	0.086	0.065	0.137	1.487	0.449	10.99	0.057	0.085	0.171	0.254	0.486	8.013	0.364	0.042	0.000		0.396	0.97
25.5	45.92	7.650	15.42	0.278	0.301	0.072	0.031	0.208	1.390	0.447	10.51	0.089	0.019	0.138	0.245	0.455	7.799	0.365	0.037	0.037		0.432	0.97
26.0	44.55	7.405	14.75	0.288	0.223	0.077	0.083	0.199	1.379	0.432	10.02	0.073	0.091	0.133	0.233	0.499	7.609	0.491	0.029	0.053	0.066	0.409	0.98
26.5	42.33	6.820	13.88	0.257	0.281	0.087	0.043	0.162	1.245	0.409	9.791	0.095	0.083	0.167	0.216	0.358	7.314	0.439	0.055	0.081	0.122	0.428	0.98
27.0	40.94	6.633	13.29	0.273	0.278	0.065	0.063	0.169	1.253	0.412	9.296	0.104	0.076	0.132	0.202	0.443	7.104	0.480	0.087	0.091	0.042	0.449	0.98
27.5	39.35	6.451	12.67	0.268	0.270	0.088	0.031	0.212	1.076	0.374	8.944	0.097	0.073	0.127	0.252	0.390	6.765	0.544	0.108	0.022	0.101	0.480	0.99
28.0	37.51	6.076	11.93	0.230	0.247	0.059	0.037	0.160	1.105	0.372	8.750	0.116	0.056	0.123	0.216	0.372	6.503	0.505	0.105	0.012	0.079	0.455	0.98
28.5	36.39	5.910	11.43	0.174	0.235	0.109	0.033	0.136	0.993	0.313	8.383	0.118	0.033	0.136	0.210	0.386	6.461	0.578	0.139	0.070	0.100	0.443	0.98
29.0	35.59	5.645	11.05	0.166	0.264	0.103	0.038	0.199	0.989	0.282	8.214	0.120	0.041	0.159	0.190	0.362	6.269	0.707	0.146	0.046	0.077	0.525	0.99
29.5	34.61	5.415	10.44	0.187	0.208	0.076	0.064	0.180	0.957	0.337	8.143	0.107	0.030	0.147	0.243	0.329	6.190	0.673	0.147	0.111	0.094	0.534	1.00
30.0	33.03	5.105	9.945	0.155	0.236	0.080	0.044	0.143	0.906	0.311	7.828	0.138	0.047	0.123	0.156	0.370	5.978	0.701	0.158	0.023	0.076	0.504	1.00
32.0	28.92	4.560	8.106	0.113	0.194	0.070	0.025	0.109	0.738	0.277	6.872	0.137	0.013	0.104	0.137	0.306	5.472	0.744	0.193	0.127	0.063	0.556	0.99

(continued on next page)

Table 2 (*continued*)

Energy (eV)	Oscillator strength (10^{-2} eV^{-1})																						η_i
	Total	Partial photoionization																					
		$C_2H_6O^+$	$C_2H_5O^+$	$C_2H_4O^+$	$C_2H_3O^+$	$C_2H_2O^+$	C_2HO^+	CH_4O^+	CH_3O^+	$C_2H_6^+$ CH_2O^+	$C_2H_5^+$ CHO^+	$C_2H_4^+$ CO^+	$C_2H_3^+$	H_2O^+	OH^+	CH_4^+ O^+	CH_3^+	CH_2^+	CH^+	C^+	H_2^+	H^+	
34.0	25.58	3.863	6.919	0.142	0.171	0.066	0.024	0.132	0.666	0.285	6.148	0.127	0.010	0.078	0.116	0.246	5.070	0.709	0.164	0.071	0.077	0.500	0.99
36.0	22.98	3.383	5.884	0.079	0.113	0.051	0.022	0.105	0.529	0.242	5.685	0.119	0.043	0.100	0.121	0.248	4.676	0.726	0.205	0.080	0.064	0.508	1.00
38.0	20.79	3.029	5.060	0.097	0.151	0.056	0.021	0.107	0.482	0.221	5.040	0.125	0.033	0.069	0.116	0.220	4.314	0.718	0.210	0.082	0.093	0.542	1.01
40.0	18.68	2.623	4.303	0.073	0.109	0.050	0.019	0.089	0.435	0.203	4.568	0.139	0.046	0.069	0.108	0.222	4.024	0.689	0.238	0.101	0.072	0.511	1.02
42.0	16.77	2.350	3.768	0.069	0.103	0.034	0.011	0.081	0.368	0.172	4.187	0.113	0.024	0.048	0.089	0.187	3.685	0.642	0.208	0.078	0.064	0.488	1.01
44.0	15.26	2.098	3.294	0.057	0.107	0.037	0.011	0.051	0.327	0.175	3.786	0.099	0.031	0.063	0.079	0.167	3.437	0.647	0.191	0.060	0.067	0.476	1.03
46.0	14.16	1.955	2.924	0.052	0.080	0.029	0.025	0.075	0.312	0.154	3.506	0.102	0.014	0.042	0.077	0.161	3.164	0.630	0.192	0.084	0.065	0.522	1.05
48.0	12.94	1.728	2.621	0.052	0.066	0.034	0.013	0.056	0.270	0.159	3.236	0.104	0.030	0.047	0.062	0.135	2.903	0.646	0.171	0.068	0.070	0.472	1.05
50.0	12.00	1.573	2.320	0.047	0.063	0.027	0.016	0.050	0.249	0.134	2.961	0.117	0.014	0.041	0.074	0.145	2.722	0.593	0.194	0.092	0.062	0.504	1.06
55.0	10.11	1.284	1.774	0.029	0.051	0.018	0.002	0.061	0.200	0.115	2.533	0.089	0.013	0.040	0.049	0.107	2.353	0.572	0.184	0.073	0.048	0.517	1.10
60.0	8.617	1.095	1.417	0.026	0.039	0.010	0.000	0.028	0.162	0.090	2.161	0.070	0.016	0.034	0.036	0.106	1.961	0.545	0.192	0.059	0.084	0.484	1.13
65.0	7.429	0.908	1.180	0.014	0.031	0.013	0.004	0.030	0.151	0.087	1.810	0.071	0.015	0.027	0.033	0.071	1.705	0.477	0.183	0.086	0.066	0.469	1.15
70.0	6.305	0.755	0.970	0.022	0.025	0.014	0.012	0.028	0.106	0.067	1.516	0.063	0.008	0.018	0.033	0.078	1.442	0.411	0.165	0.073	0.057	0.442	1.15
75.0	5.489	0.659	0.817	0.017	0.021	0.009	0.002	0.024	0.088	0.065	1.305	0.061	0.011	0.017	0.026	0.053	1.235	0.379	0.156	0.060	0.057	0.428	1.18
80.0	4.826	0.569	0.678	0.015	0.020	0.014	0.005	0.026	0.082	0.054	1.117	0.055	0.003	0.017	0.033	0.073	1.055	0.331	0.147	0.065	0.055	0.413	1.20

3.5. Partial photoionization and photofragmentation oscillator strengths

Absolute oscillator strengths for the production of the positive ion species from DME are obtained from the absolute total photoionization oscillator strengths and the photoion branching ratio at each photon energy. The results of this procedure for DME are illustrated in Figs. 7–10, which shows the partial photoionization oscillator strengths for the molecular ions and all the dissociative fragment ions ($C_2H_6O^+$, $C_2H_5O^+$, $C_2H_4O^+$, $C_2H_3O^+$, $C_2H_2O^+$, C_2HO^+ in Fig. 7; CH_4O^+, CH_3O^+, $CH_2O^+/C_2H_6^+$, $CHO^+/C_2H_5^+$, $CO^+/C_2H_4^+$, $C_2H_3^+$ in Fig. 8; H_2O^+, OH^+, CH_4^+/O^+, CH_3^+, CH_2^+, CH^+, C^+ in Fig. 9; and H_2^+, H^+ in Fig. 10) up to 80 eV. Table 2 also presents these data numerically. Earlier published relative photoionization yield curves for the dominant ion products ($C_2H_6O^+$, $C_2H_5O^+$ and CH_3^+), obtained in PIMS experiments [11], have been normalized to the presently reported absolute oscillator strengths using the $C_2H_5O^+$ data (which has the most intense yield). The resulting renormalized data [11] are shown as solid lines for comparison in Figs. 7 and 9. On this basis, the previously published PIMS data [11] for $C_2H_6O^+$ and $C_2H_5O^+$ are very similar to the presently reported data (see inserts in Fig. 7). For CH_3^+ the shapes are similar, but the fact that the data from Ref. [11] have much lower relative intensity possibly indicates discrimination against high kinetic energy ions in the PIMS study [11]. It should be noted that the ion assigned in Ref. [11] as $m/z = 31$ has an AP (13.35 eV) and an intensity that are both too large to correspond to CH_3O^+. It is possible that this ion is in fact $m/z = 29$ (i.e. $CHO^+/C_2H_5^+$), since the AP then would correspond quite closely to the values both in the present work and in other studies [36,39] as can be seen from Table 1. This conjecture is further supported by a consideration of the mass spectral intensities observed both in the present work and in NIST Chemistry WebBook mass spectral tables [46] which show that $m/z = 29$ from DME is much more intense than $m/z = 31$. Further support for this view comes from the authors statement in Ref. [11] that their data is for the four intense ions from DME. Because of these uncertainties the ioniza-

tion yield data from Ref. [11] for $m/z = 31$ has not been shown in Fig. 8. The relatively high APs for CH_2^+, CH^+, C^+, H_2^+ and H^+ (see Figs. 9 and 10) indicates that these ions are produced as a result of ionization from more tightly bound valence orbitals. In the cases of CH_2^+, CH^+ and possibly C^+, the yields increase markedly above ~27 eV which suggests that processes due to inner valence ionization and/or Coulomb explosion of multiply charged ions are contributing.

Acknowledgements

This work was financially supported by the Natural Sciences and Engineering Research Council (NSERC) of Canada.

References

[1] J.W. Gallagher, C.E. Brion, J.A.R. Samson, P.W. Langhoff, J. Phys. Chem. Ref. Data 17 (1988) 9, and references therein.
[2] R. Feng, G. Cooper, C.E. Brion, Chem. Phys. 260 (2000) 391, and references therein.
[3] H. Koizumi, K. Hironaka, K. Shinsaka, S. Arai, H. Nakazawa, A. Kimura, Y. Hatano, Y. Ito, Y. Zhang, A. Yagishita, K. Ito, K. Takana, J. Chem. Phys. 85 (1986) 4276.
[4] K. Kameta, M. Ukai, T. Kamosaki, K. Shinsaka, N. Kouchi, Y. Hatano, K. Takana, J. Chem. Phys. 96 (1992) 4911.
[5] A.J. Harrison, D.R.W. Price, J. Chem. Phys. 30 (1959) 357.
[6] R. McDiarmid, J. Chem. Phys. 60 (1974) 4091.
[7] M.B. Robin, Higher Excited States of Polyatomic Molecules, vols. I (1974), II (1975), III (1985), Academic Press, New York.
[8] M. Suto, C. Ye, L.C. Lee, J. Chem. Phys. 89 (1988) 6555.
[9] L.J. Bremner, M.G. Curtis, I.S. Walker, J. Chem. Soc. Faraday Trans. 87 (1991) 1049.
[10] K. Watanabe, J. Chem. Phys. 26 (1957) 542.
[11] R. Botter, J.M. Pechine, H.M. Rosenstock, Int. J. Mass Spectrom. Ion Phys. 25 (1977) 7.
[12] A.W. Potts, T.A. Williams, W.C. Price, Faraday Discuss. Chem. Soc. 54 (1972) 104.
[13] K. Kimura, S. Katsumata, Y. Achiba, T. Yamazaki, S. Iwata, Handbook of HeI Photoelectron Spectra of Fundamental Organic Molecules, Halsted Press, New York, 1988.
[14] G. Bieri, L. Åsbrink, W. von Niessen, J. Electron Spectrosc. Relat. Phenom. 27 (1982) 129.
[15] D.H. Aue, H.M. Webb, W.R. Davidson, M. Vidal, M.T. Bowers, H. Goldwhite, L.E. Vertal, J.E. Douglas, P.A. Kollman, G.L. Kenyon, J. Am. Chem. Soc. 102 (1980) 5151.
[16] B.J. Cocksey, J.H.D. Eland, C.J. Danby, J. Chem. Soc. B (1971) 790.
[17] M.J.S. Dewar, S.D. Worley, J. Chem. Phys. 50 (1969) 654.
[18] M. Bajic, K. Humski, L. Klasinc, B. Ruscic, Z. Naturforsch. B 40 (1985) 1214.
[19] C. Utsunomiya, T. Kobayashi, S. Nagakura, Bull. Chem. Soc. Jpn. 53 (1980) 1216.
[20] F. Carnovale, M.K. Livett, J.B. Peel, J. Am. Chem. Soc. 102 (1980) 569.
[21] T. Kobayashi, Phys. Lett. A 69 (1978) 105.
[22] F.M. Benoit, A.G. Harrison, J. Am. Chem. Soc. 99 (1977) 3980.
[23] D.H. Aue, H.M. Webb, M.T. Bowers, J. Am. Chem. Soc. 97 (1975) 4137.
[24] H. Bock, P. Mollere, G. Becker, G. Fritz, J. Organomet. Chem. 61 (1973) 113.
[25] S. Cradock, R.A. Whiteford, J. Chem. Soc. Faraday Trans. II 68 (1972) 281.
[26] A. Schweig, W. Thiel, Mol. Phys. 27 (1974) 265.
[27] D.S.C. Yee, A. Hamnett, C.E. Brion, J. Electron Spectrosc. Relat. Phenom. 8 (1976) 291.
[28] S.A.C. Clark, A.O. Bawagan, C.E. Brion, Chem. Phys. 137 (1989) 407.
[29] Y. Zheng, E. Weigold, C.E. Brion, W. von Niessen, J. Electron Spectrosc. Relat. Phenom. 53 (1990) 153.
[30] H. Koizumi, K. Shinsaka, T. Yoshimi, K. Hironaka, S. Arai, M. Ukai, M. Morita, H. Nakazawa, A. Kimura, Y. Hatano, Y. Ito, Y. Zhang, A. Yagishita, K. Ito, K. Takana, Radiat. Phys. Chem. 32 (1988) 111.
[31] K. Kameta, M. Ukai, T. Kamosaki, K. Shinsaka, N. Kouchi, Y. Hatano, K. Takana, J. Chem. Phys. 96 (1992) 4911.
[32] R.D. Bowen, A. Maccoll, Org. Mass Spectrom. 19 (1984) 379.
[33] F.P. Lossing, J. Am. Chem. Soc. 99 (1977) 7526.
[34] B.H. Solka, M.E. Russell, J. Phys. Chem. 78 (1974) 1268.
[35] C.D. Finney, A.G. Harrison, Int. J. Mass Spectrom. Ion Phys. 9 (1972) 221.
[36] A.A. Ivko, Org. Katal. (1970) 20.
[37] R.H. Martin, F.W. Lampe, R.W. Taft, J. Am. Chem. Soc. 88 (1966) 1353.
[38] M.A. Haney, J.L. Franklin, J. Chem. Soc. Faraday Trans. 65 (1969) 1794.
[39] J.J. Butler, D.M.P. Holland, A.C. Parr, R. Stockbauer, Int. J. Mass Spectrom. Ion Processes 58 (1984) 1.
[40] R. Feng, G. Cooper, C.E. Brion, Chem. Phys. 244 (1999) 127, and references therein.
[41] R. Feng, G. Cooper, C.E. Brion, Chem. Phys. 249 (1999) 223, and references therein.
[42] R. Feng, G. Cooper, C.E. Brion, Chem. Phys. 252 (2000) 359, and references therein.

[43] R. Feng, G. Cooper, Y. Sakai, C.E. Brion, Chem. Phys. 255 (2000) 353, and references therein.
[44] G. Cooper, Y. Zheng, G.R. Burton, C.E. Brion, Rev. Sci. Instrum. 64 (1993) 1140.
[45] S.G. Lias, J.E. Bartmess, J.F. Liebman, J.L. Holmes, R.D. Levin, W.G. Mallard, J. Phys. Chem. Ref. Data (Suppl. 17) (1988) 1.
[46] NIST Mass Spec Data Center, S.E. Stein (Director), IR and Mass Spectra, in: W.G. Mallard, P.J. Linstrom (Eds.), NIST Chemistry WebBook, NIST Standard Reference Database Number 69, February 2000, National Institute of Standards and Technology, Gaithersburg MD, 20899 (http://webbook.nist.gov).